

Reinforced embankments over soft foundations under undrained and partially drained conditions

R. Kerry Rowe*, Allen Lunzhu Li

Department of Civil and Environmental Engineering, University of Western Ontario, London, Ontario, Canada N6A 5B9

Received 23 October 1998; received in revised form 27 November 1998; accepted 9 December 1998

Abstract

The behaviour of geosynthetic reinforced embankments constructed on soft cohesive foundations under undrained and partially drained conditions is examined using an elliptical cap soil model. Consolidation is modelled using Biot theory. The effects of reinforcement stiffness, partial consolidation of the foundation soil during embankment construction and foundation soils with different initial undrained strength profiles are examined. Particular attention is focused on the strains in the geosynthetic reinforcement at working conditions and at embankment failure. The effect of reinforcement on the deformation of the foundation soil is evaluated. It is shown that reinforcement can significantly reduce the maximum lateral deformations, vertical deformation and foundation soil heave during embankment construction. For the conditions examined, partial drainage during construction provides an 11–38% increase in the factor of safety against failure of reinforced embankments relative to that expected under perfectly undrained conditions. © 1999 Elsevier Science Ltd.

Keywords: Embankment; Soft soil; Reinforcement; Partial drainage; Consolidation

1. Introduction

The undrained behaviour of reinforced embankments constructed over soft clay foundations has been extensively investigated using the Mohr–Coulomb and Modified Cam–clay models to describe foundation soil behaviour (Rowe and Soderman, 1987a, 1987b; Hird et al., 1990). In addition, several researchers (e.g. Chai and Bergado, 1993; Litwinowicz et al., 1994; Rowe et al., 1996) have used effective stress

*Corresponding author. Tel.: (519) 661-2126; fax: (519) 661-3942; e-mail: r.k.rowe@uwo.ca
Dr. N.W.M. John acted as Special Editor for this paper.

analysis methods to model the behaviour of several case histories. However, the effect of reinforcement on the construction of embankments over foundations under partially drained conditions has received very little attention. The objective of this paper is to theoretically investigate the behaviour of embankments during both undrained and partially drained construction to identify and highlight the effect of geosynthetic reinforcement and partial consolidation of foundation soils during embankment construction. Particular attention will be given to the effect of partial consolidation on the expected stability of geosynthetic reinforced embankments.

2. Numerical model and problem considered

The finite element program AFENA (Carter and Balaam, 1990) was modified to incorporate a soil model with an elliptical cap (see Fig. 1; Chen and Baladi, 1985; Chen and Mizuno, 1990) for both undrained and transient conditions, using coupled Biot consolidation theory for the transient case. The elliptical cap undrained model has been applied to describe the undrained behaviour of Boston blue clay under an MIT test embankment loading (McCarron and Chen, 1987). Rowe and Hinchberger used an elasto-viscoplastic cap model to successfully predict the time-dependent behaviour

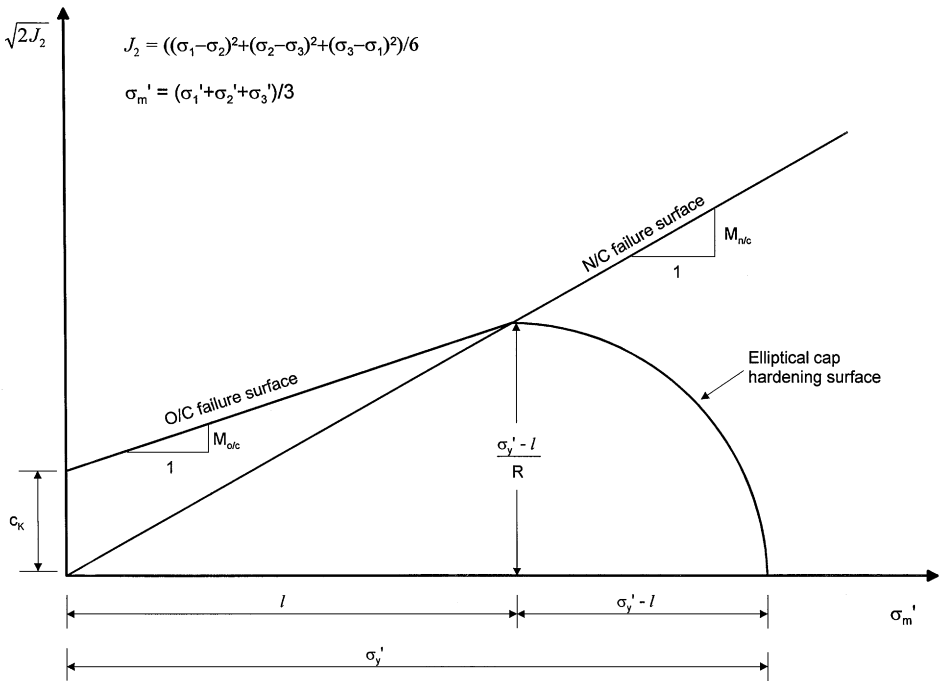


Fig. 1. Elliptical cap soil model adopted (see also Table 1) (modified from Chen and Mizuno, 1990).

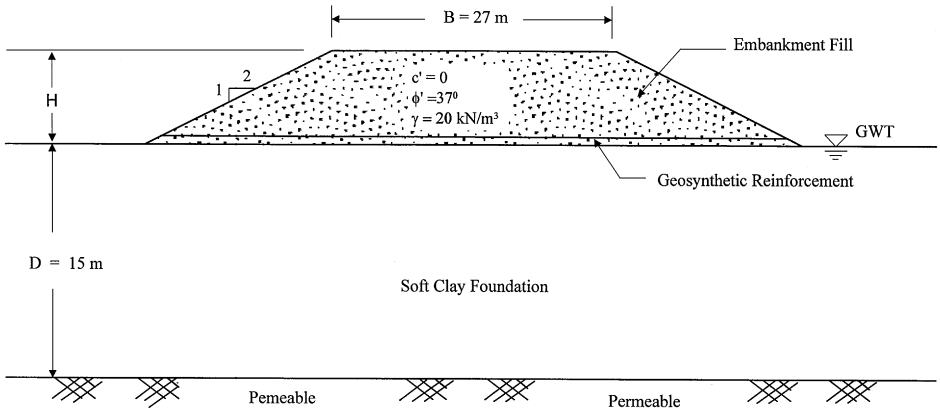


Fig. 2. Reinforced embankment and foundation.

of both the reinforced Sackville test embankment (Rowe and Hinchberger, 1998) and unreinforced Gloucester test embankment (Hinchberger and Rowe, 1998).

In this present study, the construction of a four-lane highway embankment (see Fig. 2) with 27 m crest width and 2(horizontal):1(vertical) side slopes was examined. The soft foundation was taken to be 15 m deep and underlain by a relatively permeable layer. The water table was assumed to be at ground level and the initial pore pressures prior to embankment construction were taken to be hydrostatic. The centreline of the embankment (a line of symmetry) and the far field lateral boundary were taken to be smooth and rigid with the lateral boundary located 100 m from the centreline. The bottom of the finite element mesh was assumed to be rough and rigid. A total of 1969 linear strain triangular elements (4357 nodes) were used to discretize the embankment and foundation soils. Two noded bar elements were used for modeling the reinforcement and two noded joint elements were used for both the embankment fill/reinforcement interface and the embankment fill/foundation interface (Rowe and Soderman, 1987a). Embankment construction was simulated by placing 0.75 m thick lifts such that the body forces were applied using between 200 to 600 incremental load steps depending on the stage of construction.

3. Model parameters

3.1. Selection of foundation soil properties

Two typical soft clays were examined. Soil A has a liquid limit of 76% and a plasticity index of 40% while Soil B has a liquid limit of 48% and a plasticity index of 30%. The preconsolidation pressure, σ'_p , profiles are shown in Fig. 3. Soil B has a higher preconsolidation pressure than Soil A. Both clays were slightly overconsolidated with an OCR of 1.1–2.6 and 1.1–2.9, respectively below the first two

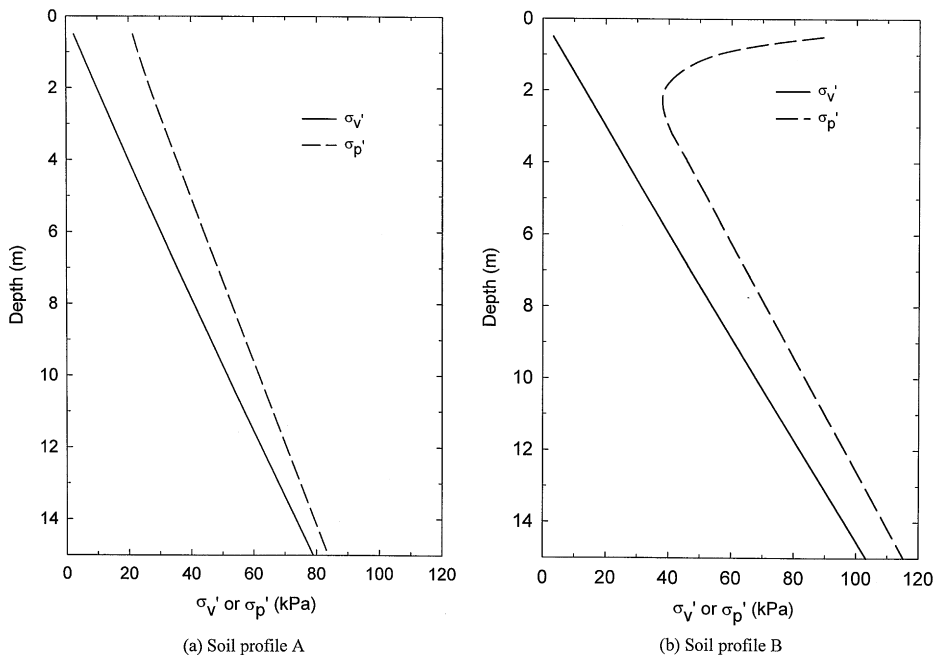


Fig. 3. Preconsolidation profiles of foundation soils A and B.

metres. Soil B has 2 meter crust that is heavily overconsolidated. Other soil parameters are summarized in Table 1. The aspect ratio of hardening elliptical cap, R , was based on typical limit state curves for natural soft clays (Leroueil, 1997). The initial void ratio and unit weight of this clay deposit at ground surface was taken to be 2.5 and 14.7 kN/m^3 for Soil A, and 1.5 and 16.5 kN/m^3 for Soil B. The variation in unit weight and void ratio with depth were taken to be consistent with the initial void ratio and unit weight at the ground surface, the preconsolidation pressure profile and the compression and the recompression indices. Thus the calculated saturated unit weight increased with depth from 14.7 kN/m^3 to 15.6 kN/m^3 for Soil A and from 16.5 kN/m^3 to 16.9 kN/m^3 for Soil B. Using these parameters, for the first soil profile the undrained shear strength s_{uo} at surface was 5 kPa and the rate of increase in undrained strength with depth, ρ_c , was 1.5 kPa/m. For the second soil profile s_{uo} was 20 kPa at surface, decreased to 10 kPa at 2 metre depth, and then increased with depth at a rate of 2.0 kPa/m. Soil A has an undrained shear strength profile similar to that of a soft clay in Queensland, Australia (Litwinowicz et al., 1994), while Soil B has an undrained shear strength profile much like that of Malaysian Muar clay (Chai and Bergado, 1993).

Consolidation of soft clays involves a decrease in void ratio and hydraulic conductivity and they can be related by

$$k_v = Ak_{v0} \exp\left(\frac{e - e_0}{C_k}\right), \quad (1)$$

Table 1

Elliptical cap soil model parameters (see also Fig. 1) and constants to describe the variation of hydraulic conductivity with consolidation and loading in Eq. (1)

	Soil A	Soil B
Elliptical cap model parameters:		
Failure envelope $M_{n/c}$	0.874	0.91
Friction angle (N/C)	27°	28°
Cohesion intercept for N/C clay c_k	0.0	0.0
Failure envelope $M_{o/c}$	0.63	0.75
Cohesion intercept for O/C clay c_k (kPa)	2.7–4.7	3.4–6.3
Aspect ratio R	0.7	1.25
Compression index λ	0.3	0.15
Recompression index κ	0.03	0.025
Coefficient of earth pressure at rest K'_0	0.6	0.6
Poisson's ratio ν'	0.35	0.35
Hydraulic conductivity parameters:		
k_{vo} (m/s)	1×10^{-9}	1×10^{-9}
e_o	2.5	1.5
C_k	0.5	0.5
$A_{n/c}$	1	1
$A_{o/c}$	10	10
k_h/k_v	3	3

where k_{vo} is the reference hydraulic conductivity; C_k is the hydraulic conductivity change index; e_o is the reference void ratio; A is hydraulic conductivity factor; and the values adopted for these parameters are summarized in Table 1. A value of $A = 10$ in the over consolidated stage reducing to $A = 1$ in the normally consolidated state reflects the fact that in the over consolidated portion of loading the hydraulic conductivity may be substantially higher than in the normally consolidated state (Leroueil et al., 1978a, 1978b). The ratio of horizontal to vertical hydraulic conductivity $k_h/k_v = 3$ was selected to consider anisotropy of the hydraulic conductivity as observed by Tavenas et al. (1983) and noted by Terzaghi et al. (1996).

3.2. Embankment fill parameters

The embankment fill was assumed to be a purely frictional granular soil with a friction angle $\phi' = 37^\circ$, dilatancy angle $\psi = 6^\circ$, and a unit weight $\gamma = 20 \text{ kN/m}^3$. The non-linear elastic behaviour of the fill was modelled using Janbu's (1963) equation:

$$(E/P_a) = K(\sigma_3/P_a)^m, \quad (2)$$

where E is the Young's modulus of the soil; P_a is the atmospheric pressure; σ_3 is the minor principal stress; and K and m are material constants selected to be 100 and 0.5, respectively based on tests on sandy fill material used in a reinforced embankment (Rowe et al., 1984).

3.3. Interface parameters and reinforcement stiffness

Elastoplastic joint elements (Rowe and Soderman, 1987a) were used to model the fill/reinforcement interface and fill/foundation interface. The fill/reinforcement interface was fictional with $\phi' = 37^\circ$. The fill/foundation interface had the same shear strength as that of the foundation soil at the ground surface (e.g. $s_{uo} = 5$ kPa in undrained analyses and $c' = 0$, and $\phi' = 27^\circ$ in coupled analyses for Soil A). Reinforcement with tensile stiffness, J , varying from 0 (no reinforcement) to 8000 kN/m was examined.

4. Results and discussion

4.1. Effect of reinforcement for undrained conditions

The undrained elliptical cap soil model was used to examine the behaviour of reinforced embankments over two soft foundations (A and B) for undrained conditions. The calculated variation of the embankment failure height with reinforcement stiffness for embankments constructed over foundation Soils A and B is presented in Fig. 4 and the corresponding calculated maximum strains in the reinforcement are given in Fig. 5. The failure height, H_f , is defined as the fill thickness corresponding to

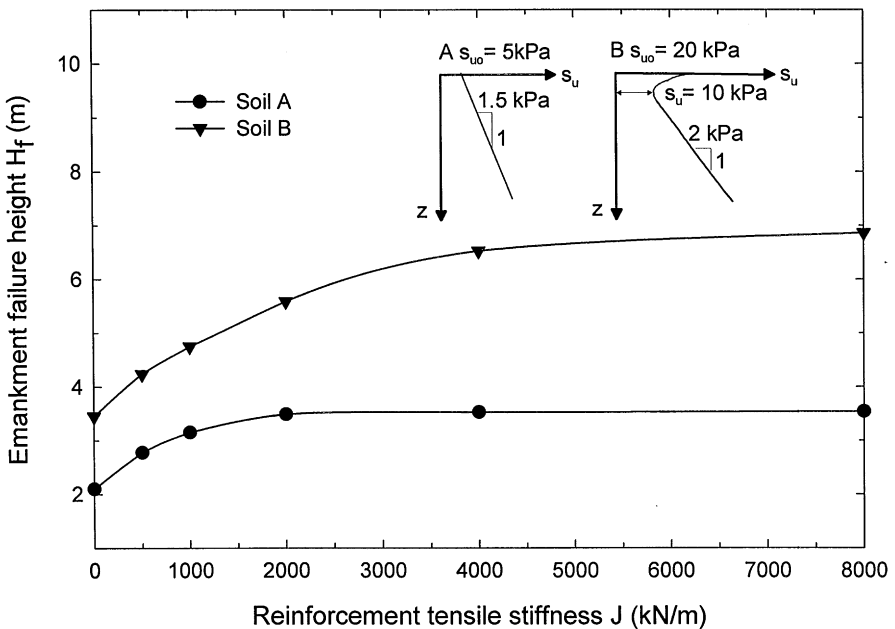


Fig. 4. Embankment failure height vs. reinforcement tensile stiffness: undrained conditions.

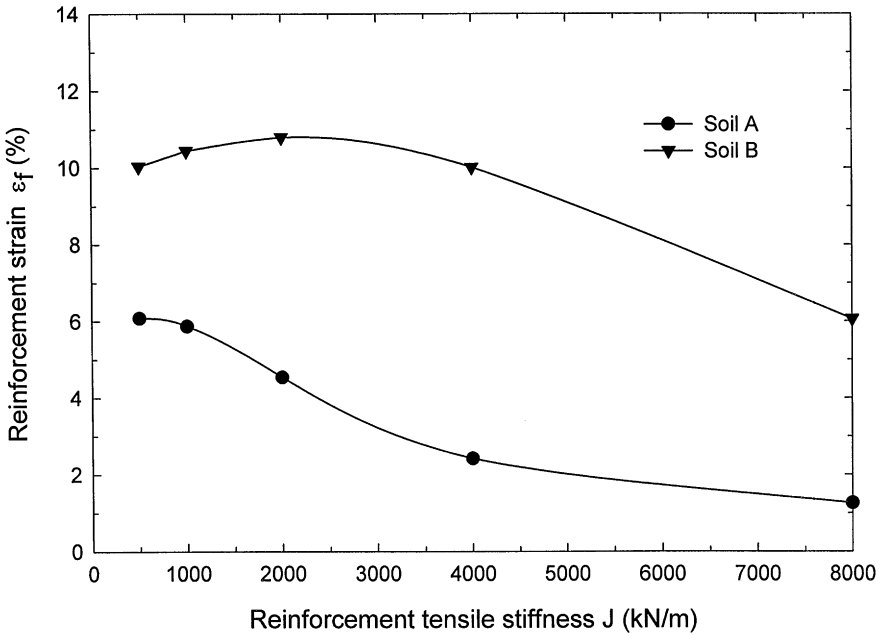


Fig. 5. Reinforcement strain at embankment failure: undrained conditions.

the maximum net embankment height (Rowe and Soderman, 1987a). The unreinforced embankment failure height was 2.1 m and 3.45 m for foundation Soils A and B, respectively. For Soil A, a change of reinforcement stiffness from 500 kN/m to 8000 kN/m resulted in an increase in failure height by between 0.68 m to 1.44 m relative to the unreinforced case. The effect of reinforcement on the embankment failure height was most significant where J increases from 500 kN/m to 2000 kN/m. Within this range of reinforcement stiffness, the embankments were under-reinforced. For J greater than 2000 kN/m, the embankments were over-reinforced and increasing reinforcement stiffness no longer influenced the stability. For Soil B, the change of reinforcement stiffness from $J = 500$ kN/m to 8000 kN/m resulted in an increase in failure height by between 0.79 m and 3.41 m relative to the unreinforced case. The embankments were under-reinforced up to $J = 4000$ kN/m and hence the effect of increasing reinforcement tensile stiffness was significant up to $J = 4000$ kN/m. The results indicated that the effect of reinforcement was substantially greater for the embankments over the stronger foundation than for those over the weaker foundation under the ideal undrained conditions considered. These findings are consistent with earlier finding by Rowe and Soderman (1987b).

Supposing that the analyses reported in Figs. 4 and 5 were conducted using the expected (unfactored) soil parameters, then, H_f shown in Fig. 4 represents the failure height as controlled by the foundation and foundation-reinforcement interaction assuming that the reinforcement has sufficient strength to sustain the tensile force

developed in the reinforcement. This force can be related the strain in the reinforcement at failure of the embankment, ϵ_f , which was up to 6% and 10.5% for Soils A and B, respectively. The effect of limiting the allowable strain in the reinforcement to either 4% or 6% are shown for soil profiles A and B, in Figs. 6 and 7. For soil profile A (Fig. 6), the strain ϵ_f was less than or equal to 6% for all J and hence the embankment height H_e is the same as the failure height for this case. Adopting a limiting strain of 4% reduces the embankment height H_e for $J \leq 2000$ kN/m. For soil profile B (Fig. 7) limiting the strain to either 4% or 6% reduced the height H_e to which the embankment could be constructed for $J < 8000$ kN/m (i.e. most practical cases).

Under working conditions embankments will typically have a factor of safety greater than one and the reinforcement strain will be significantly lower than the strain at embankment failure given in Fig. 5. Assuming a factor of safety of 1.3 against foundation failure for undrained conditions, Fig. 8 shows the variation of calculated maximum reinforcement strain, ϵ_T , under working conditions for a range of reinforcement stiffnesses, J . The reinforcement strain was below 5% for both soil profiles examined. Although the embankments have the same factor of safety of 1.3, the mobilized reinforcement strains tended to increase with tensile stiffness when embankments were under-reinforced (see Fig. 4) and to decrease with J when embankments were over-reinforced. However, the mobilized reinforcement tensile force increased monotonically with increasing embankment height under working conditions.

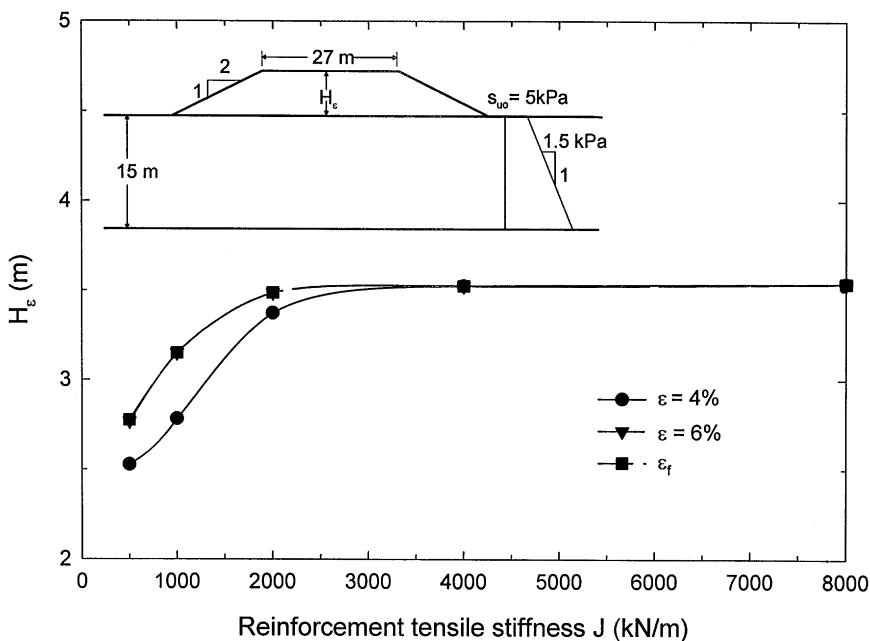


Fig. 6. H_e vs. J for soil A under undrained conditions.

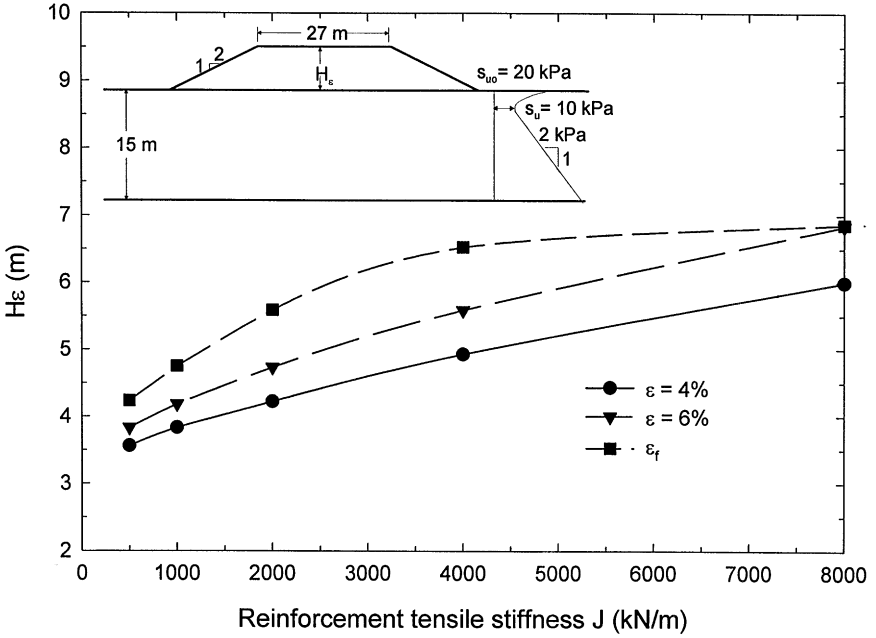


Fig. 7. H_ϵ vs. J for soil B under undrained conditions.

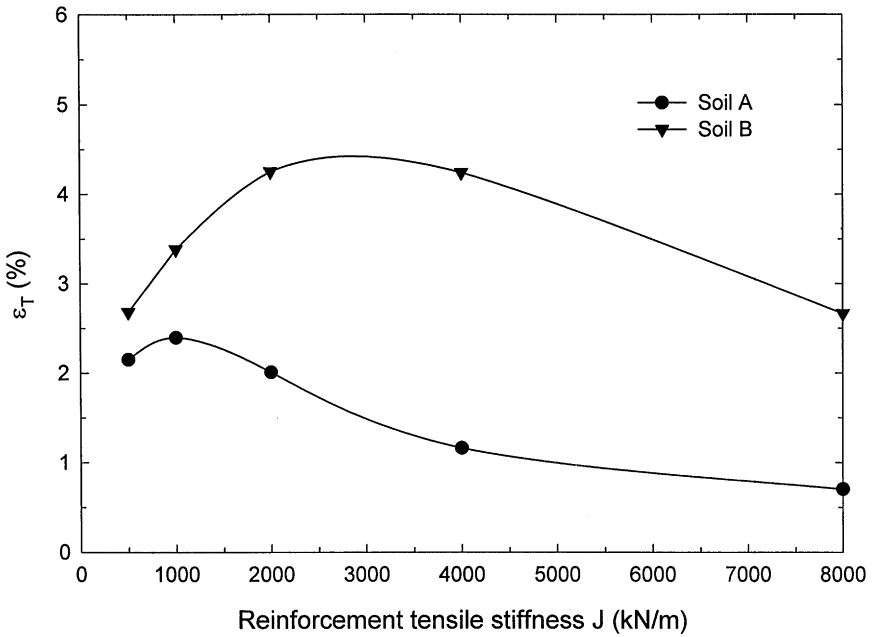


Fig. 8. Reinforcement strain ϵ_T under working conditions (undrained).

4.2. Effect of reinforcement for partially drained conditions

Recognizing that most real soils are initially overconsolidated and that the soil layers near the ground surface and any underlying permeable deposit will experience some consolidation during embankment construction, the analyses reported in the previous section were repeated using a fully coupled analysis to examine the behaviour of embankments under partially drained conditions using a single stage construction sequence. A construction rate of 0.85 m/month was used and the upper and lower surfaces of the clay layers were assumed to be free draining boundaries. The effect of the partial consolidation during construction can be partly assessed by examining the embankment settlement and excess pore pressures. For example, for Soil A, $J = 8000$ kN/m and a fill thickness of 3.6 m, the calculated immediate undrained settlement was 9.3 cm while the total partially drained settlement was 21.8 cm at the end of construction. Fig. 9 shows pore pressure ratio $B = \Delta u / \Delta \sigma$ (where $\Delta \sigma = (\Delta \sigma_1 + \Delta \sigma_2 + \Delta \sigma_3) / 3$) for Soil B with $J = 4000$ kN/m at fill thickness $H = 1.5$ m. This also represents the ratio of excess pore pressure under partially drained conditions to the excess pore pressure under undrained conditions. As can be seen significant partial consolidation of the foundation soil occurred during the first 1.5 m embankment construction and this is consistent with field observation (e.g. Leroueil et al., 1978a, b; Rowe et al., 1996). Of even greater interest is the effect of the increase in shear strength due to the consolidation on the stability of the reinforced embankment to be discussed below.

Fig. 10 shows the calculated embankment failure heights under partially drained conditions for Soils A and B. The unreinforced embankment failure height of 2.44 m and 4.2 m for cases A and B respectively were 16% and 22% higher than that for the undrained case. A change of reinforcement stiffness from 500 kN/m to 8000 kN/m resulted in an increase in failure height by between 0.71 m to 2.36 m relative to the

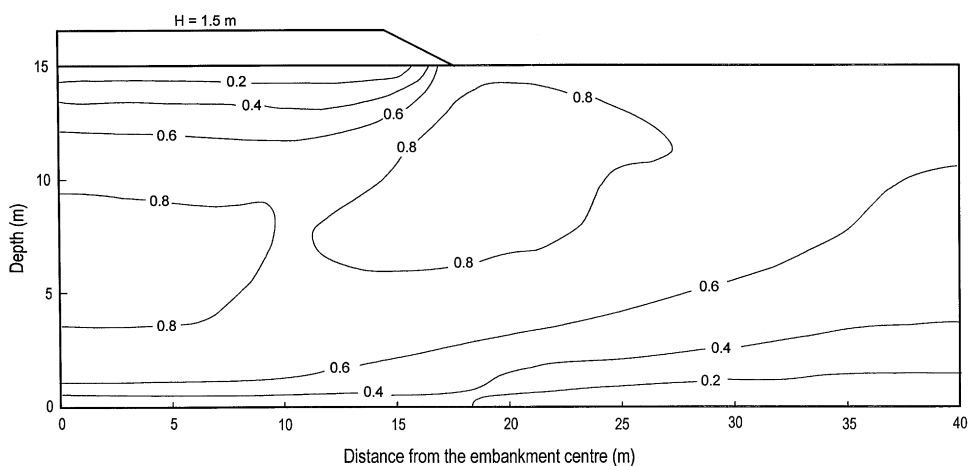


Fig. 9. The contour of ratio $B = \Delta u / \Delta \sigma_m$.

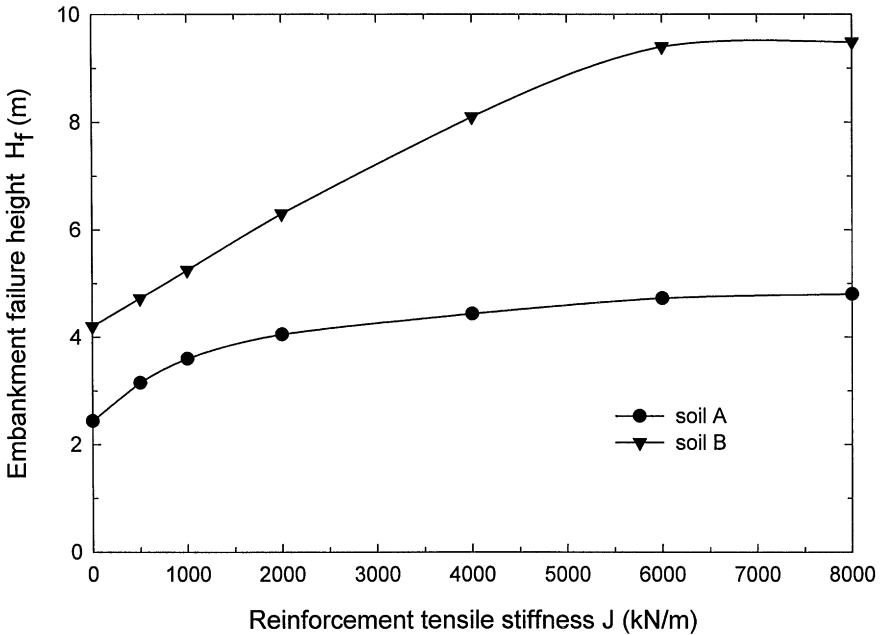


Fig. 10. Embankment failure height vs. reinforcement tensile stiffness: partially drained conditions.

unreinforced case for Soil A and the increase in reinforcement stiffness had a significant effect on the embankment failure height up to $J = 2000$ kN/m. For Soil B, the change of reinforcement stiffness from $J = 500$ kN/m to 8000 kN/m resulted in an increase in failure height by between 0.53 m 5.29 m relative to the unreinforced case and the increase in reinforcement tensile stiffness had a significant effect on stability up to $J = 6000$ kN/m. Comparing Fig. 4 and Fig. 10, it can be seen that reinforcement has a greater effect for partially drained cases than for undrained cases. Similar to the undrained cases, the reinforcement has a greater effect for the stronger foundation than the weaker foundation.

Fig. 11 shows the calculated maximum reinforcement strain at embankment failure, ϵ_f , for both soils and a range of tensile stiffness, assuming that the reinforcement can sustain these strains without reinforcement failure. For Soil A, ϵ_f was between 3.2% and 6.5%. For Soil B, much higher reinforcement strains were mobilized at embankment failure (3.1% and 14.7%) because substantially higher embankments were constructed. If one was to limit embankment height, H_ϵ , based on an allowable reinforcement strain ϵ of 4% or 6%, then the maximum embankment height would be as given in Figs 12 and 13 for Soils A and B, respectively. For Soil A, the effect of limiting the reinforcement strain is modest, however, for Soil B the embankment height is controlled by the permissible strain. Nevertheless, even for the most conservative case ($\epsilon \leq 4\%$) comparison of Figs. 6–12 and Figs. 7–13 shows that partial drainage during construction still considerably increases the height to which the embankment can be constructed.

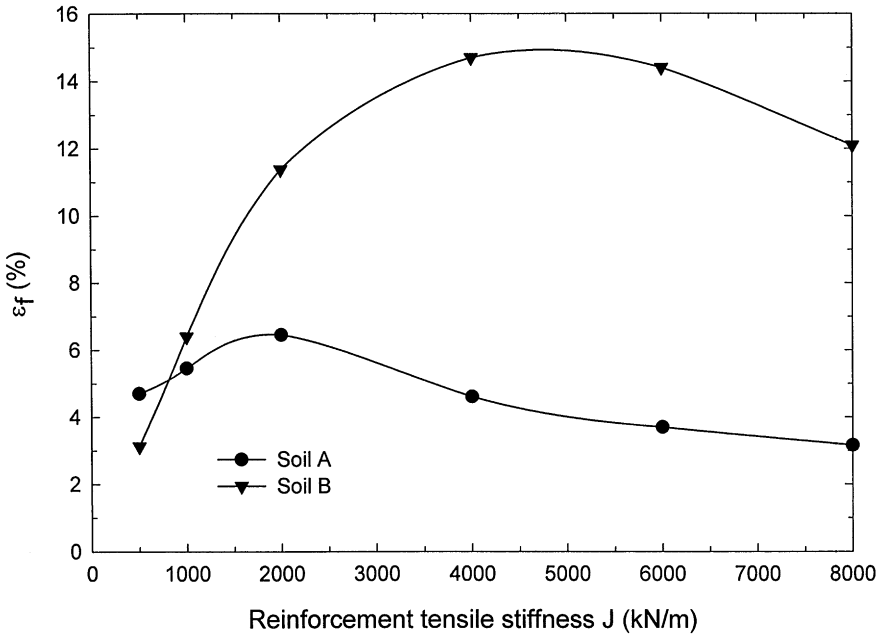


Fig. 11. Reinforcement strain at failure: partially drained conditions.

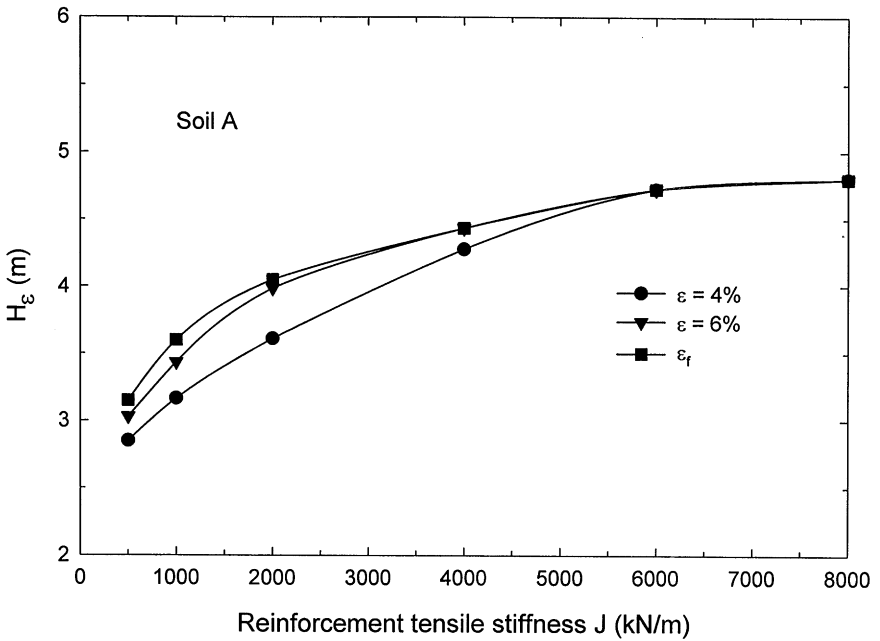


Fig. 12. H_ϵ at different reinforcement strain vs. tensile stiffness J .

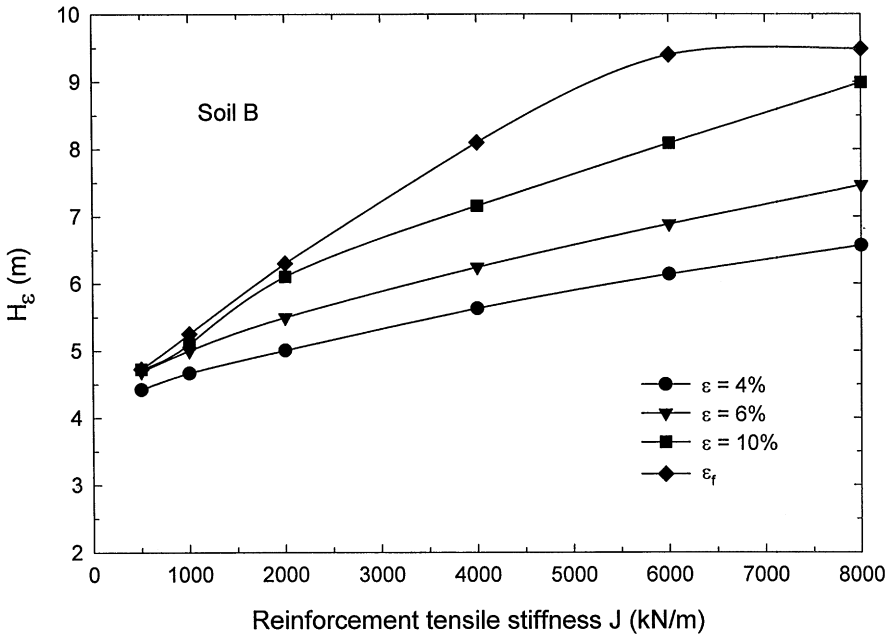


Fig. 13. H_{ε} at different reinforcement strain vs. tensile stiffness J .

If the design of embankment was based on undrained conditions (without any limit due to permissible strain) using a factor of safety of 1.3 against foundation failure, the reinforcement strain at working condition (ε_T) allowing for partial consolidation during construction were less than 2.5% for both soil profiles as indicated in Fig. 14. If the permissible reinforcement strain was 6%, the reinforcement strain at working condition (ε_{TB}) were less than 1.9% for both soil profiles shown in Fig. 14 (note that the strain $\varepsilon_{TB} = \varepsilon_T$ for Soil A). Consequently, the mobilized reinforcement tensile forces would be relatively small. This, in part, shows why the observed field strains under working condition are typically so low (e.g. Fowler and Edris Jr., 1987; Fritzinger, 1990; Litwinowicz et al., 1994). Fig. 14 also shows that the maximum reinforcement strain ε_{fu} if the embankments were constructed to the height at which undrained failure would be predicted (but allowing for partial dissipation of pore pressure during construction). In this case, the maximum reinforcement strain was in the range of 1%–4% and 3%–6.5% for Soils A and B, respectively. Thus even at the undrained failure height these embankments would be expected to be stable provided that the reinforcement can sustain these strains.

4.3. Distribution of reinforcement strain and deformation under partially drained conditions

Fig. 15 shows the variation in calculated reinforcement strain with distance from the centre of embankment at the point of embankment failure for Soil A. For

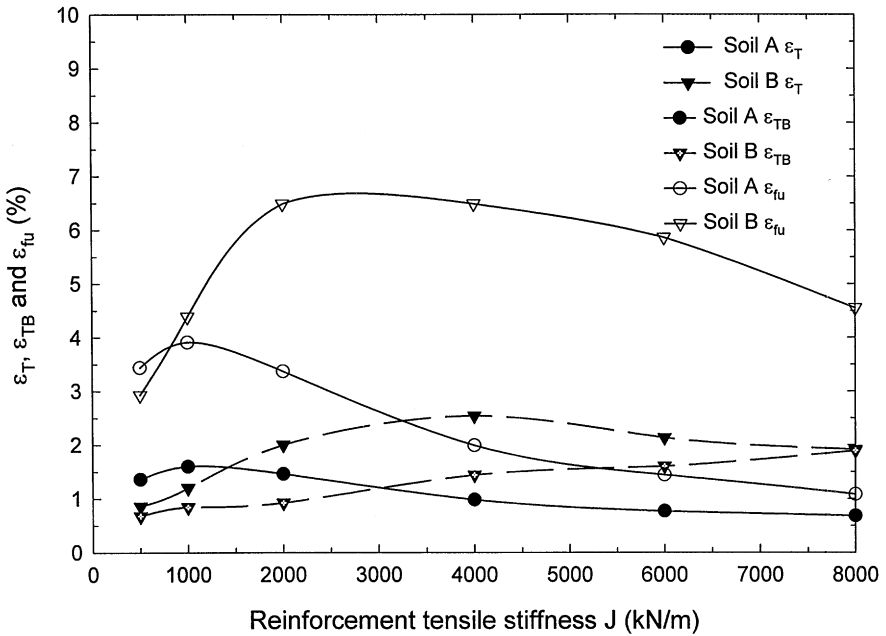


Fig. 14. Reinforcement strain ϵ_T , ϵ_{TB} and ϵ_{fu} : partially drained conditions.

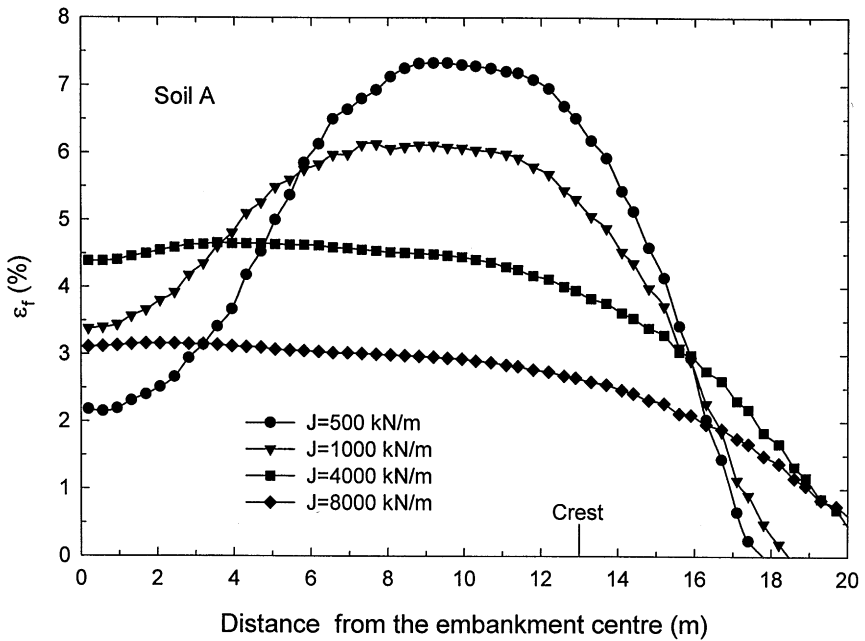


Fig. 15. Reinforcement strain at failure ϵ_f .

$J = 500$ kN/m, the maximum strain was located at 9.2 m away from the centre of the embankment. The location of maximum reinforcement strain gradually moved towards the centre line as J increased from 500 kN/m to 8000 kN/m. This reflects a change in failure mechanism. A similar trend was found for Soil B.

Fig. 16 shows the calculated maximum deformation at the end of construction for embankments under partially drained conditions. The change of stiffness from 500 kN/m to 4000 kN/m significantly decreases the maximum horizontal displacement, maximum vertical displacement and heave. The effect of reinforcement was more significant for the stronger foundation, especially the reduction in heave.

5. Implications

From the undrained and fully coupled analysis of embankments constructed over the two soft foundations, it can be seen that partially drained conditions may substantially increase the failure height of reinforced embankments due to the shear strength gain of the foundation soil during embankment construction. This is particularly noteworthy when high stiffness reinforcement is used. In many field cases (Leroueil et al., 1978a, b) it has been shown that the foundation soil will experience significant partial consolidation during the early stage of embankment loading. Thus the assumption of undrained conditions is potentially quite conservative for soils that are even slightly overconsolidated prior to loading.

If the embankment design is based on undrained analyses, the factor of safety is underestimated for these soils. Comparing Figs 4 and 10, it can be seen that the ratio of failure height H_f under partially drained condition to the failure height H_f under undrained conditions (for both soil profiles examined and a range of tensile stiffness for the reinforcement) is similar and varies between 1.1 to 1.4. Thus the partially drained condition inherently provides a factor of safety 1.1 to 1.4 relative to undrained failure heights for these soil profiles and construction conditions. As indicated in Fig. 14, the maximum reinforcement strain at working conditions for the cases considered, ε_{Tmax} , was below 2.5% for embankment designed based on undrained stability.

6. Conclusions

The results from both an undrained analysis and fully coupled analysis that accounts for partial dissipation of excess pore water pressure during construction have been presented. These results suggest that for the range of conditions and soils examined:

1. Geosynthetic reinforcement can substantially increase the stability of embankments on the soft foundations under both undrained and partially drained conditions.
2. When typical construction rates and partial pore pressure dissipation during construction were considered, the excess pore pressure developed in the foundation

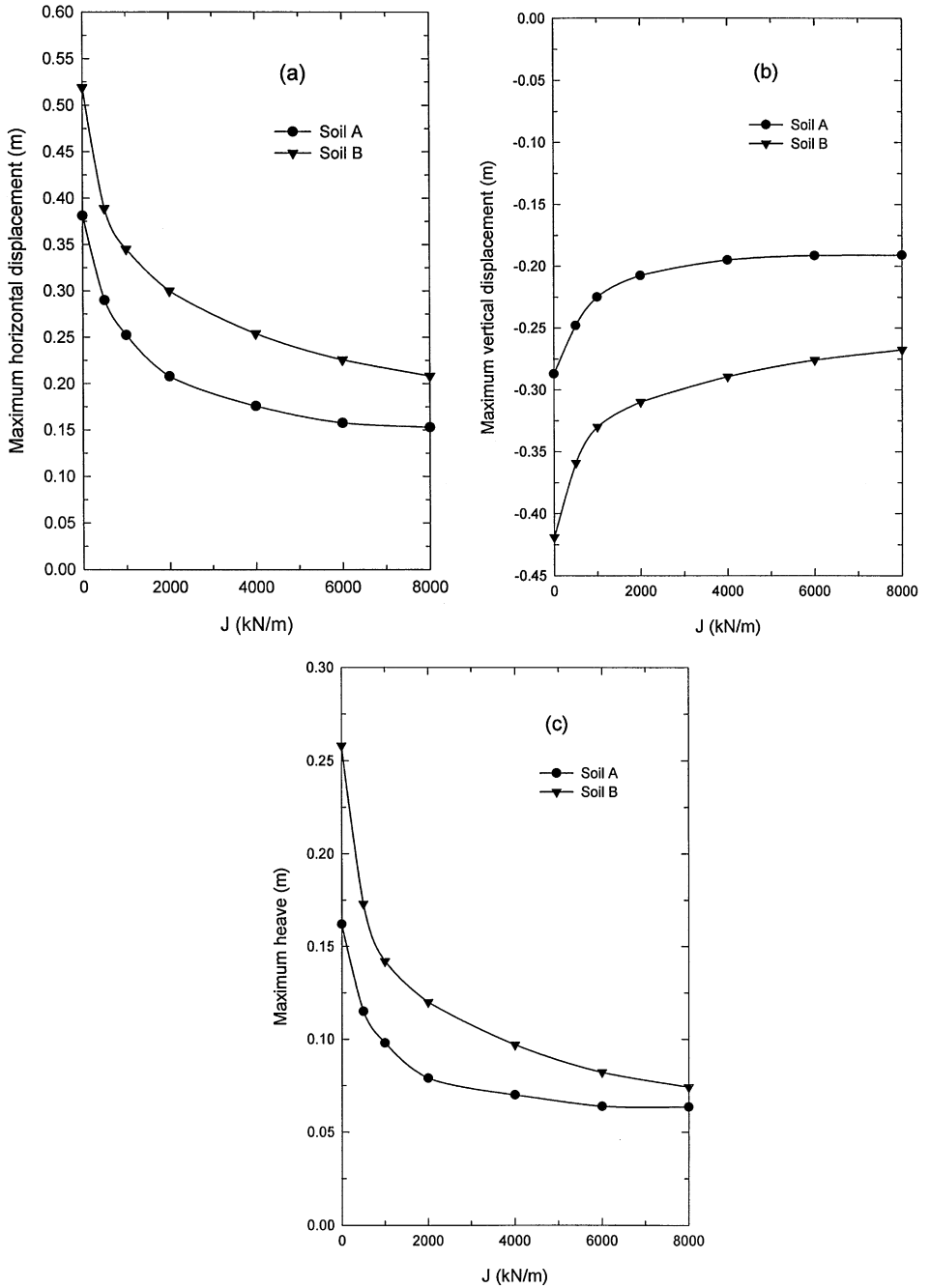


Fig. 16. The variation of maximum horizontal, vertical and heave displacement with reinforcement stiffness.

soil at the end of construction was substantially less than that expected under undrained conditions.

3. The effect of stiff reinforcement was greater under partially drained conditions than under undrained conditions. This was, in part, due to the increase of strength near the soil reinforcement interface allowing greater mobilization of the reinforcing force.
4. Partially drained conditions inherently provide a factor of safety 1.1 to 1.4 against undrained failure of the reinforced embankments examined. Under partially drained conditions the reinforcement strain at the failure height predicted for undrained conditions was less than 7%.
5. Reinforcement was predicted to reduce the vertical and lateral shear deformations beneath the embankment crest and reduce the heave at the toe during embankment construction.

Acknowledgement

The research reported in the paper was funded by the Natural Sciences and Engineering Research Council of Canada.

References

- Carter, J.P., Balaam, N.P., 1990. AFENA – A general finite element algorithm: users manual. School of Civil and Mining Engineering, University of Sydney, NSW 2006, Australia.
- Chai, J., Bergado, D.T., 1993. Performance of reinforced embankment on Muar clay deposit. *Soils and Foundations* 33 (4), 1–17.
- Chen, W.F., Baladi, G.Y., 1985. *Soil plasticity: theory and implementation*. Elsevier, Amsterdam.
- Chen, W.F., Mizuno, E., 1990. *Nonlinear analysis in soil mechanics – theory and implementation*. Elsevier, New York.
- Fowler, J., Edris Jr, E.V., 1987. fabric reinforced embankment test section. Plaquemine Parish, Louisiana, USA. *Geotextiles and Geomembranes* 6, 1–31.
- Frizinger, S.A., 1990. Subaqueous use of high-strength geotextiles. 4th International Conference on Geotextiles and Geomembranes and Related Products, The Hague, Netherlands, 1990, Vol. 1, pp. 143–148.
- Hinchberger, S.D., Rowe, R.K., 1998. Modelling the rate sensitive characteristics of the Gloucester foundation soil. *Canadian Geotechnical Journal* 35 (in press).
- Hird, C.C., Pyrah, I.C., Russel, D., 1990. Finite element analysis of the collapse of reinforced embankments on soft ground. *Geotechnique* 40 (4), 633–640.
- Janbu, N., 1963. Soil compressibility as determined by oedometer and triaxial tests. *Proceedings of the European Conference on Soil Mechanics and Foundation Engineering, Wiesbaden, Germany, Vol. 1*, pp. 19–25.
- Leroueil, S., Tavenas, F., Trak, B., La Rochelle, P., Roy, M., 1978a. Construction pore pressures in clay foundations under embankments. Part I: the Sanint-Alban test fills. *Canadian Geotechnical Journal* 15 (1), 52–65.
- Leroueil, S., Tavenas, F., Mieussens, C., Peignaud, M., 1978b. Construction pore pressures in clay foundations under embankments. Part II: generalized behaviour. *Canadian Geotechnical Journal* (15) (1) 65–82.

- Leroueil, S., 1997. Critical state soil mechanics and the behaviour of real soils. Proceedings of the International Symposium on Recent Developments in Soil and Pavement Mechanics, Rio de Janeiro, Brazil, June, in: *Recent Developments in Soil and Pavement Mechanics*, A.A. Balkema/Rotterdam/Brookfield, pp. 41–80.
- Litwinowicz, A., Wijeyakulasuriya, C.V., Brandon, A.N., 1994. Performance of a reinforced embankment on a sensitive soft clay foundation. Fifth International Conference on Geotextiles, Geomembranes and Related Products, Singapore, September, Vol. 1, pp. 11–16.
- McCarron, W.O., Chen, W.F., 1987. A capped plasticity model applied to Boston blue clay. *Canadian Geotechnical Journal* 24 (4), 630–644.
- Rowe, R.K., Maclean, M.D., Soderman, K.L., 1984. Analysis of a geotextile reinforced embankment constructed on peat. *Canadian Geotechnical Journal* 21 (3), 563–576.
- Rowe, R.K., Soderman, K.L., 1987a. Very soft soil stabilization using high strength geotextiles: The role of finite element analysis. *International Journal of Geotextiles and Geomembranes* 6, 53–81.
- Rowe, R.K., Soderman, K.L., 1987b. Reinforcement of embankments on soils whose strength increases with depth. *Proceedings of Geosynthetics '87*, New Orleans, pp. 266–277.
- Rowe, R.K., Gnanendran, C.T., Landva, A.O., Valsangkar, A.J., 1996. Calculated and observed behaviour of a reinforced embankment over soft compressible soil. *Canadian Geotechnical Journal* 33 (2), 324–338.
- Rowe, R.K., Hinchberger, S.D., 1998. The significance of rate effects in modelling the Sackville test embankment. *Canadian Geotechnical Journal* 35 (3), 500–516.
- Tavenas, F., Jean, P., Leblond, P., Leroueil, 1983. The permeability of natural soft clays. Part II: Permeability characteristics. *Canadian Geotechnical Journal* 20 (4), 645–660.
- Terzaghi, K., Peck, R.B., Mesri, G., 1996. *Soil mechanics in engineering practice*. Wiley, New York.